

# Hydrogen acts as a therapeutic antioxidant by selectively reducing cytotoxic oxygen radicals

Ikuroh Ohsawa<sup>1</sup>, Masahiro Ishikawa<sup>1</sup>, Kumiko Takahashi<sup>1</sup>, Megumi Watanabe<sup>1,2</sup>, Kiyomi Nishimaki<sup>1</sup>, Kumi Yamagata<sup>1</sup>, Ken-ichiro Katsura<sup>2</sup>, Yasuo Katayama<sup>2</sup>, Sadamitsu Asoh<sup>1</sup> & Shigeo Ohta<sup>1</sup>

Acute oxidative stress induced by ischemia-reperfusion or inflammation causes serious damage to tissues, and persistent oxidative stress is accepted as one of the causes of many common diseases including cancer. We show here that hydrogen (H<sub>2</sub>) has potential as an antioxidant in preventive and therapeutic applications. We induced acute oxidative stress in cultured cells by three independent methods. H<sub>2</sub> selectively reduced the hydroxyl radical, the most cytotoxic of reactive oxygen species (ROS), and effectively protected cells; however, H<sub>2</sub> did not react with other ROS, which possess physiological roles. We used an acute rat model in which oxidative stress damage was induced in the brain by focal ischemia and reperfusion. The inhalation of H<sub>2</sub> gas markedly suppressed brain injury by buffering the effects of oxidative stress. Thus H<sub>2</sub> can be used as an effective antioxidant therapy; owing to its ability to rapidly diffuse across membranes, it can reach and react with cytotoxic ROS and thus protect against oxidative damage.

Oxidative stress arises from the strong cellular oxidizing potential of excess reactive oxygen species (ROS), or free radicals<sup>1–5</sup>. Most of the superoxide anion radical (O<sub>2</sub><sup>•</sup>) produced is generated in mitochondria by electron leakage from the electron transport chain and the Krebs cycle<sup>6</sup>. O<sub>2</sub><sup>•</sup> is also produced by metabolic oxidases, including NADPH oxidase and xanthine oxidase<sup>7</sup>. Superoxide dismutase converts O<sub>2</sub><sup>•</sup> into hydrogen peroxide (H<sub>2</sub>O<sub>2</sub>)<sup>8</sup>, which is detoxified into H<sub>2</sub>O by either glutathione peroxidase or catalase. Excess O<sub>2</sub><sup>•</sup> reduces transition metal ions such as Fe<sup>3+</sup> and Cu<sup>2+</sup> (ref. 2), the reduced forms of which in turn can react with H<sub>2</sub>O<sub>2</sub> to produce hydroxyl radicals (•OH) by the Fenton reaction. •OH is the strongest of the oxidant species and reacts indiscriminately with nucleic acids, lipids and proteins. There is no known detoxification system for •OH; therefore, scavenging •OH is a critical antioxidant process<sup>9</sup>.

Despite their cytotoxic effects, O<sub>2</sub><sup>•</sup> and H<sub>2</sub>O<sub>2</sub> play important physiological roles at low concentrations: they function as regulatory signaling molecules that are involved in numerous signal transduction cascades and also regulate biological processes such as apoptosis, cell proliferation and differentiation<sup>7,10</sup>. At higher concentrations, H<sub>2</sub>O<sub>2</sub> is converted into hypochlorous acid by myeloperoxidase; hypochlorous acid defends against bacterial invasion<sup>5</sup>. Nitric oxide (NO•), another ROS, functions as a neurotransmitter and is essential for the dilation of blood vessels<sup>11</sup>. Thus, cytotoxic radicals such as •OH must be neutralized without compromising the essential biological activities of other, physiologically beneficial, ROS. Here we demonstrate that molecular hydrogen (dihydrogen, H<sub>2</sub>) can alleviate •OH-induced cytotoxicity without affecting the other ROS, and propose that H<sub>2</sub> has potential as an antioxidant for preventive and therapeutic applications.

## RESULTS

### H<sub>2</sub> selectively reduces •OH in cultured cells

H<sub>2</sub> reduces the •OH that is produced by radiolysis or photolysis of water<sup>12</sup>; however, whether H<sub>2</sub> can effectively neutralize •OH in living cells has not been directly investigated. As the cellular damage produced by spontaneous generation of •OH is not sufficient to be detectable, we induced O<sub>2</sub><sup>•</sup> production in PC12 cultured cells. To do this, we treated the cells with a mitochondrial respiratory complex III inhibitor, antimycin A (ref. 13); following such treatment, O<sub>2</sub><sup>•</sup> in these cells is rapidly converted into H<sub>2</sub>O<sub>2</sub>. The addition of antimycin A increased levels of O<sub>2</sub><sup>•</sup> and H<sub>2</sub>O<sub>2</sub>, as judged by the fluorescence signals emitted by the oxidized forms of MitoSOX (Fig. 1a) and 2',7'-dichlorodihydrofluorescein (H<sub>2</sub>DCF) (Supplementary Fig. 1 online), respectively. We dissolved H<sub>2</sub> and O<sub>2</sub> into medium as described in the Methods, and confirmed the prolonged (24 h long) maintenance of H<sub>2</sub> levels (Supplementary Fig. 2 online). H<sub>2</sub> dissolved in culture medium did not decrease MitoSOX and DCF signals in the cells (Fig. 1a,b and Supplementary Fig. 1). Additionally, H<sub>2</sub> did not decrease the steady-state level of NO• (Supplementary Fig. 1). In contrast, H<sub>2</sub> treatment significantly decreased levels of •OH, as assessed by the fluorescence signal emitted by the oxidized form of 2-[6-(4'-hydroxy)phenoxy-3H-xanthen-3-on-9-yl] benzoate (HPF) (refs. 14,15 and Fig. 1c,d). When we exposed the cells to antimycin A (30 μg/ml) in the absence of H<sub>2</sub>, the HPF signals increased in both the nuclear region and the cytoplasm, probably because H<sub>2</sub>O<sub>2</sub> diffused from the mitochondria to produce •OH. Notably, H<sub>2</sub> decreased •OH levels even in the nuclear region (Fig. 1c).

<sup>1</sup>Department of Biochemistry and Cell Biology, Institute of Development and Aging Sciences, Graduate School of Medicine, Nippon Medical School, 1-396 Kosugi-cho, Nakahara-ku, Kawasaki City 211-8533, Japan. <sup>2</sup>Department of Internal Medicine, Nippon Medical School, 1-1-5 Sendagi, Bunkyo-ku, Tokyo 113-8602, Japan. Correspondence should be addressed to S.O. (ohta@nms.ac.jp).

Received 25 September 2006; accepted 15 March 2007; published online 7 May 2007; doi:10.1038/nm1577

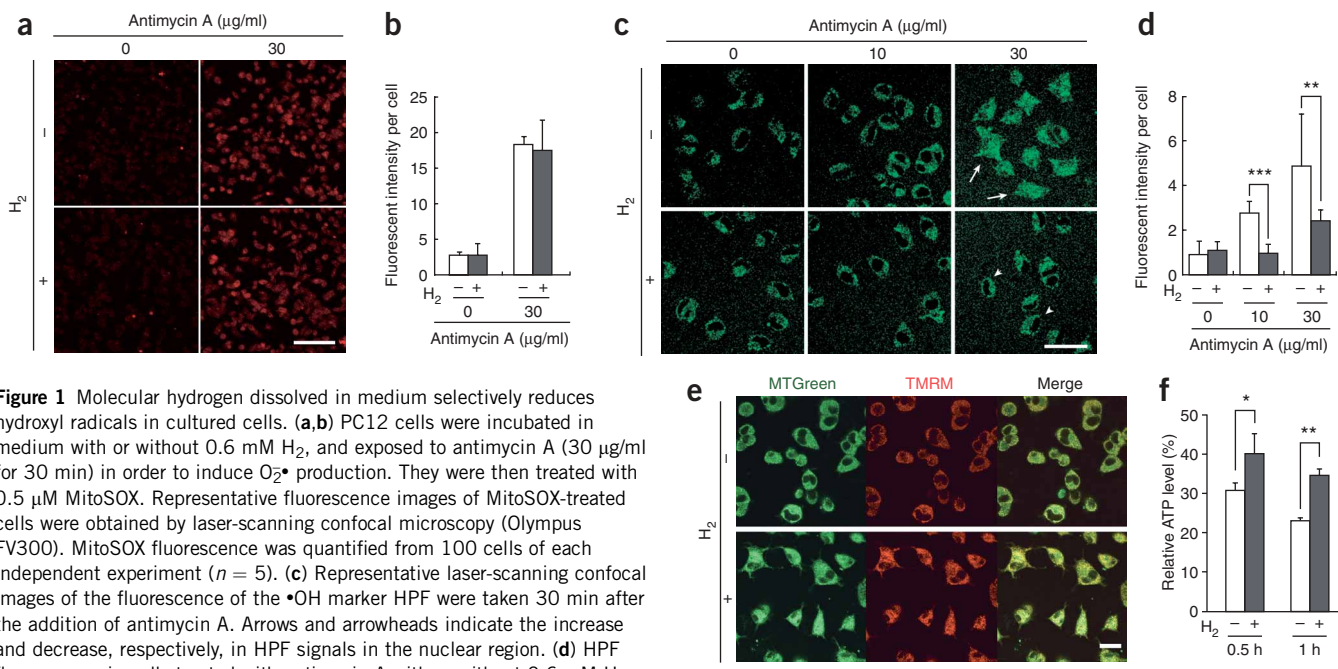


**Figure 1** Molecular hydrogen dissolved in medium selectively reduces hydroxyl radicals in cultured cells. **(a,b)** PC12 cells were incubated in medium with or without 0.6 mM  $H_2$ , and exposed to antimycin A (30  $\mu\text{g/ml}$ ) for 30 min in order to induce  $O_2^{\bullet}$  production. They were then treated with 0.5  $\mu\text{M}$  MitoSOX. Representative fluorescence images of MitoSOX-treated cells were obtained by laser-scanning confocal microscopy (Olympus FV300). MitoSOX fluorescence was quantified from 100 cells of each independent experiment ( $n = 5$ ). **(c)** Representative laser-scanning confocal images of the fluorescence of the  $\bullet\text{OH}$  marker HPF were taken 30 min after the addition of antimycin A. Arrows and arrowheads indicate the increase and decrease, respectively, in HPF signals in the nuclear region. **(d)** HPF fluorescence in cells treated with antimycin A with or without 0.6 mM  $H_2$  was quantified from 100 cells ( $n = 4$ ).  $^{**}P < 0.01$ ,  $^{***}P < 0.001$ . **(e)** At 30 min after adding antimycin A (10  $\mu\text{g/ml}$ ) with or without  $H_2$  (0.6 mM), cells were incubated with 1  $\mu\text{M}$  MTGreen and 100 nM TMRM for 10 min and then imaged. The two images were superimposed (merge). **(f)** Cells were pretreated with 4.5 g/l 2-deoxy-D-glucose (an inhibitor of glycolysis) and 1 mM pyruvate, and relative cellular ATP levels were quantified after exposure to 30  $\mu\text{g/ml}$  antimycin A. ATP levels of cells not treated with antimycin A were set at 100% ( $n = 3$ ).  $^*P < 0.05$ ,  $^{**}P < 0.01$ . Scale bars: 100  $\mu\text{m}$  in **a**; 50  $\mu\text{m}$  in **c**; 20  $\mu\text{m}$  in **e**. Histograms show mean  $\pm$  s.d.

After antimycin A treatment,  $H_2$  prevented the decline of the mitochondrial membrane potential, as detected by fluorescence of tetramethylrhodamine methyl ester (TMRM), which depends upon the mitochondrial membrane potential, whereas fluorescence levels of MitoTracker Green (MTGreen), which are independent of the membrane potential, were unchanged (**Fig. 1e**). This suggested that  $H_2$  protected mitochondria from  $\bullet\text{OH}$ .  $H_2$ -treated cells looked normal, whereas  $H_2$ -untreated cells were shrunken and had abnormal round shapes (**Fig. 1e**). Along with this protective effect,  $H_2$  also prevented a decrease in the cellular levels of ATP synthesized in mitochondria (**Fig. 1f**). The fact that  $H_2$  protected mitochondria and nuclear DNA provided evidence that  $H_2$  penetrated most membranes and diffused into organelles.

### $H_2$ dissolved in medium protects cultured cells against $\bullet\text{OH}$

We placed PC12 cells in culture medium containing  $H_2$  and  $O_2$ , and, at the same time, induced oxidative stress by adding antimycin A. At 24 h after the induction of ROS with antimycin A, we observed that  $H_2$  seemed to protect nuclear DNA from oxidation, as shown by decreased levels of oxidized guanine (8-OH-G) (**Fig. 2a,b** and ref. 16). Moreover,  $H_2$  also decreased levels of 4-hydroxyl-2-nonenal (HNE), an end-product of lipid peroxides (**Fig. 2c,d** and ref. 17), indicating that it protected lipids from peroxidation. Further,  $H_2$  dissolved in medium protected cells from cell death in a dose-dependent manner (**Fig. 2e,f**). When we removed  $H_2$  from medium that had been saturated with  $H_2$ , the protective effect disappeared (**Fig. 2f**), suggesting that the observed effect was not due to a reaction of  $H_2$  with the medium. Moreover, we confirmed that  $H_2$  protected cellular viability by using two methods: a modified MTT assay (WST-1 assay) and measurement of cellular lactate dehydrogenase (LDH) leakage from damaged cells (**Supplementary Fig. 3** online). To exclude the possibility that the protective effect of  $H_2$  was due to a reaction with

antimycin A, we induced ROS by adding menadione, an inhibitor that acts on mitochondrial complex I, and observed that  $H_2$  protected cells in this system as well (**Supplementary Fig. 3**).

To verify that  $H_2$  protects against  $\bullet\text{OH}$ , we pretreated cells with  $\text{Cu}^{2+}$  and then exposed them to ascorbate, in order to reduce intracellular  $\text{Cu}^{2+}$  to  $\text{Cu}^+$ , which in turn catalyzes the production of  $\bullet\text{OH}$  from cellular  $\text{H}_2\text{O}_2$  that is endogenously produced. This treatment primarily induced  $\bullet\text{OH}$  inside the cells (by the Fenton reaction), thus directly confirming that  $H_2$  protects cells against cellular  $\bullet\text{OH}$  (**Fig. 2g,h**).

### Spin-trapping identifies a free radical that is reduced by $H_2$

To identify the free radical species that  $H_2$  reduces, we studied the effects of  $H_2$  on electron spin resonance (ESR) signals of spin-trapping reagents. We produced  $\bullet\text{OH}$  by the cellular Fenton reaction, and semiquantified the cellular levels of  $\bullet\text{OH}$  by spin-trapping using 5,5-dimethyl-1-pyrroline *N*-oxide (DMPO). Measurements of ESR indicated that  $H_2$  treatment did indeed decrease signals of  $\bullet\text{DMPO-OH}$  derived from  $\bullet\text{OH}$  (**Fig. 3a-c**).

Moreover, when we induced  $O_2^{\bullet}$  production by treating cells with antimycin A in the presence of DMPO, we observed multiple ESR signals<sup>18</sup>. These signals seemed to consist of those from the  $\bullet\text{DMPO-OH}$  and  $\bullet\text{DMPO-H}$  radicals (**Fig. 3d-f**). The  $\bullet\text{DMPO-H}$  radical is derived from the hydrogen radical ( $\text{H}^{\bullet}$ ), which can be induced by porphyrins. To visualize the signals decreased by  $H_2$ , we obtained the differential spectrum. We found that only  $\bullet\text{OH}$ -derived signals were decreased by  $H_2$  treatment (**Fig. 3e**). These results strongly suggest the selective reduction of cellular  $\bullet\text{OH}$  by  $H_2$  treatment.

### $H_2$ selectively reduces $\bullet\text{OH}$ and $\text{ONOO}^-$ in cell-free systems

Next, we confirmed in a pure solution that HPF fluorescence can be used to monitor the reduction of  $\bullet\text{OH}$  by  $H_2$  during continuous  $\bullet\text{OH}$

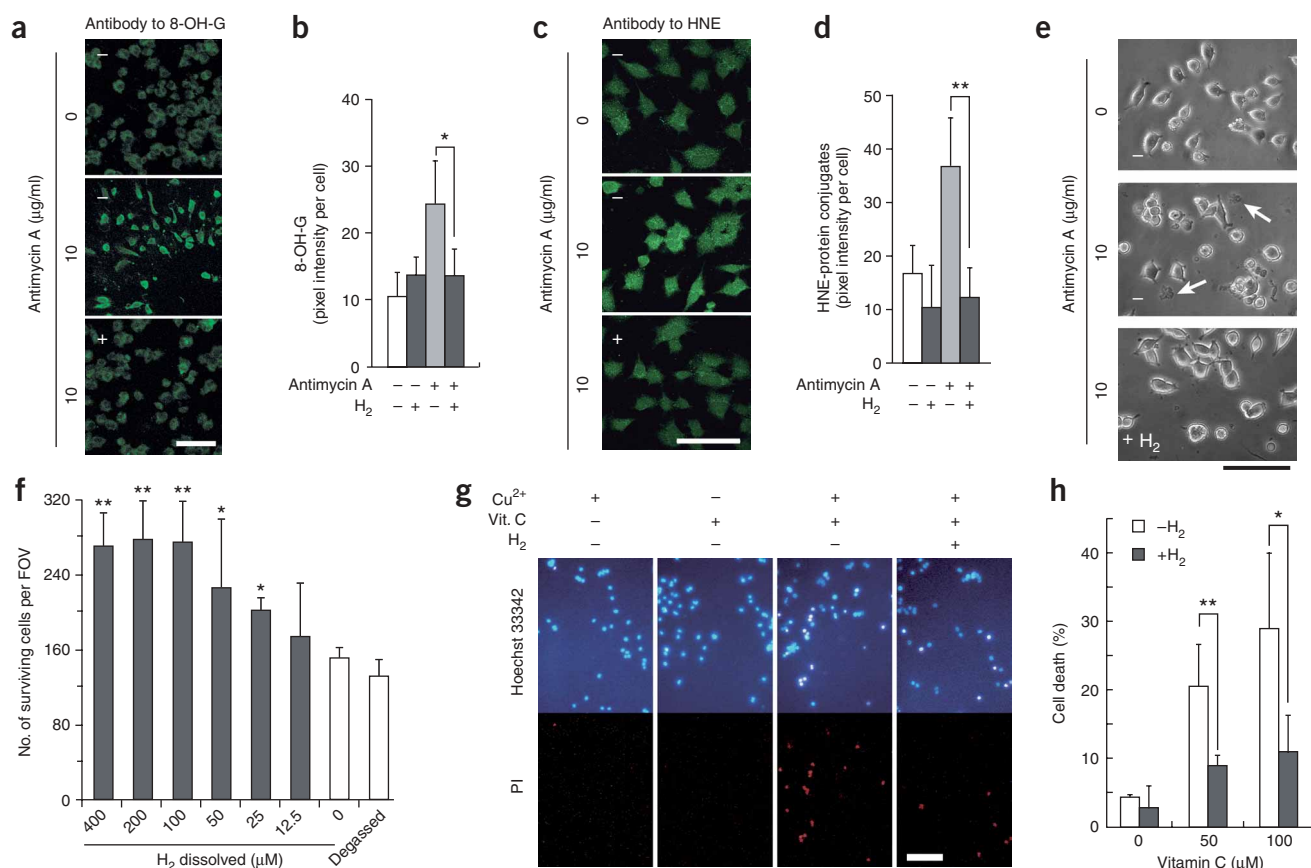


**Figure 2** Molecular hydrogen protects cultured PC12 cells by scavenging hydroxyl radicals. (**a–d**) PC12 cells were maintained with 10 μg/ml antimycin A, with (+) or without (–) 0.6 mM H<sub>2</sub>, for 24 h in a closed flask, and immunostained with antibodies to 8-OH-G or HNE. Fluorescence signals in response to 8-OH-G and HNE were quantified using 100 cells from each independent experiment ( $n = 4$ ). \* $P < 0.05$ , \*\* $P < 0.01$ . (**e**) Phase-contrast pictures of PC12 cells 24 h after the exposure to antimycin A, with (+) or without (–) 0.6 mM H<sub>2</sub>. Arrows indicate dead cells. (**f**) Cell survival was assessed by manually counting the cells (Methods;  $n = 4$ ). \* $P < 0.05$ , \*\* $P < 0.01$  (compared with 0 μM H<sub>2</sub>). (**g**) PC12 cells were exposed to intracellular •OH produced by the Fenton reaction, with or without 0.6 mM H<sub>2</sub>. Cells were preincubated with 1 mM CuSO<sub>4</sub>, washed, and exposed for 1 h to 0.1 mM ascorbate (Vit. C) in order to reduce intracellular Cu<sup>2+</sup> to Cu<sup>+</sup> (Supplementary Methods). The cells were costained with propidium iodide (PI) (for dead cells) and Hoechst 33342 to visualize the nuclei. (**h**) Cell survival was assessed by manually counting the cells as in **f** ( $n = 5$ ). \* $P < 0.05$ , \*\* $P < 0.01$ . Scale bars: 50 μm in **a,c,e**; 100 μm in **g**. Histograms represent mean ± s.d.

production by the Fenton reaction. In this condition, H<sub>2</sub> suppressed increases in HPF signals in a dose-dependent manner (Fig. 4a–c). But when we mixed a solution containing H<sub>2</sub> with HPF preoxidized with •OH, fluorescence signals from oxidized HPF did not decrease (data not shown), supporting the idea that H<sub>2</sub> directly reacts with •OH.

Next, we examined the reactivity of H<sub>2</sub> with other ROS or reactive nitrogen species (RNS). We prepared H<sub>2</sub>O<sub>2</sub> and peroxynitrite (ONOO<sup>–</sup>) by dilution of the respective stock solutions, O<sub>2</sub>•<sup>–</sup> by the enzymatic reaction of xanthine oxidase with xanthine, and NO• by the spontaneous reaction of 1-hydroxy-2-oxo-3-(*N*-methyl-3-aminopropyl)-3-methyl-1-triazene (NOC7) in cell-free systems (Supplementary Methods online). H<sub>2</sub> reduced ONOO<sup>–</sup> (Fig. 4d) somewhat, but did not reduce H<sub>2</sub>O<sub>2</sub>, NO• and O<sub>2</sub>•<sup>–</sup> (Fig. 4e–g). In cell-free experiments, we examined whether H<sub>2</sub> reduced the oxidized forms of biomolecules involved in metabolic oxidation-reduction reactions. At room temperature and neutral pH, solutions saturated with H<sub>2</sub> did not reduce the oxidized form of nicotinamide adenine dinucleotide (NAD<sup>+</sup>), the oxidized form of flavin adenine dinucleotide (FAD) or the oxidized form of cytochrome C (data not shown). Thus we infer that H<sub>2</sub> does not affect the metabolism involved in oxidation-reduction

reactions or the levels of O<sub>2</sub>•<sup>–</sup>, H<sub>2</sub>O<sub>2</sub>, and NO•, all of which play essential roles in signal transduction.

### H<sub>2</sub> protects neurons from *in vitro* ischemia and reperfusion

We also induced oxidative stress in a primary culture of neocortical cells<sup>19</sup> under more physiological conditions. It is known that rapid transition from an ischemic condition to reperfusion results in oxidative stress damage<sup>20</sup>. To mimic ischemia, we subjected neocortical cells to oxygen glucose deprivation (OGD) under nitrogen or hydrogen gas for 60 min, followed by reperfusion with medium containing O<sub>2</sub> and glucose.

HPF fluorescence showed that 10 min after the completion of OGD followed by reperfusion, •OH levels notably increased when H<sub>2</sub> was absent, but diminished when H<sub>2</sub> was present (Supplementary Fig. 4 online). At 24 h after OGD and reperfusion, H<sub>2</sub> increased neuron survival and vitality (Supplementary Fig. 4), indicating that H<sub>2</sub> protects neurons against oxidative stress-induced cell death.

### Inhalation of H<sub>2</sub> gas protects brain injury by reperfusion

To examine the therapeutic applicability of H<sub>2</sub> as an antioxidant, we used a rat model of ischemia. ROS are generated during cerebral

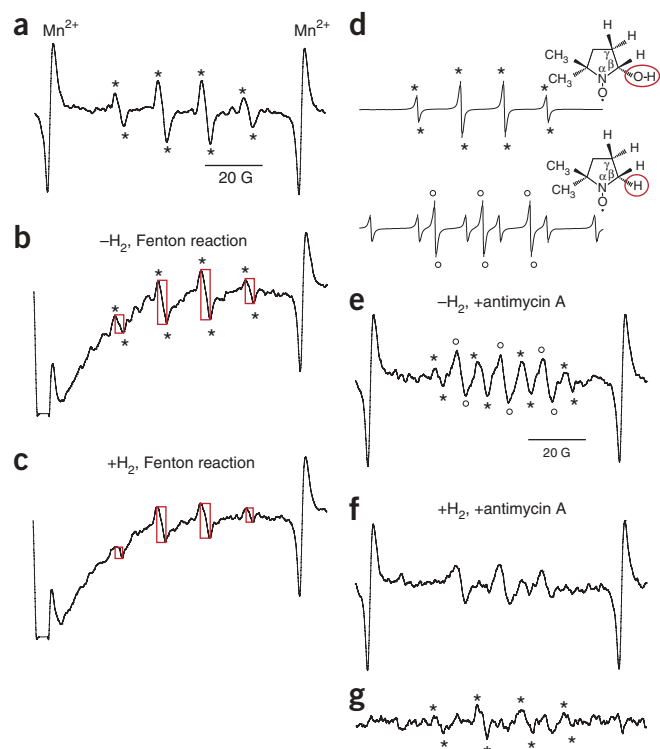


**Figure 3** Spin-trapping identifies the free radical species that  $H_2$  reduces. (a) Standard electron spin resonance (ESR) signals of the  $\bullet$ DMPO-OH radical were obtained by trapping  $\bullet$ OH with a spin-trapping reagent (DMPO; details in **Supplementary Methods**). (b,c) PC12 cells were preincubated with 0.1 M DMPO and 2 mM  $CuSO_4$  for 30 min at 37 °C with or without 0.6 mM  $H_2$ . After removal of this medium, the cells were treated with 0.2 mM ascorbate and 0.1 mM  $H_2O_2$  for 5 min at 23 °C to produce  $\bullet$ OH and then scraped into a flat cuvette for ESR measurement. Rectangle height reflects signal intensity. (d) The  $\bullet$ DMPO-OH and  $\bullet$ DMPO-H radicals<sup>18</sup> and their corresponding ESR signals are illustrated. (e,f) PC12 cells were incubated in PBS containing 0.1 M DMPO and 30  $\mu$ g/ml antimycin A for 7 min at 23 °C, with or without 0.6 mM  $H_2$ , then scraped into a flat cuvette for ESR measurement. (g) A differential spectrum was obtained by subtracting the spectrum in f from that in e, in order to visualize the signals decreased by  $H_2$  treatment. \* indicates  $\bullet$ DMPO-OH signals derived from  $\bullet$ OH. \* and o indicate  $\bullet$ DMPO-OH and  $\bullet$ DMPO-H signals, respectively (a, b, d, e and g).

as measured by the Doppler effect (ref. 24 and **Supplementary Fig. 5** online).  $H_2$  dissolved in arterial blood was increased by the inhalation of  $H_2$  in proportion to the concentration inhaled; the amount of  $H_2$  dissolved in venous blood was less than that in artery blood, suggesting that  $H_2$  had been incorporated into tissues (**Fig. 5a**).

At 1 d after MCA occlusion, we sectioned and stained brains with 2,3,5-triphenyltetrazolium chloride (TTC), a substrate for mitochondrial respiration (**Fig. 5b**). We estimated infarct volumes by assessing the staining of brain areas (white indicates infarct, **Fig. 5b,c**), and found a clear  $H_2$ -dependent decrease in infarct volume, with 2–4% of  $H_2$  providing the most substantial effect (**Fig. 5c**). We also noted that  $H_2$  exerted its effect only when it was inhaled during reperfusion; when  $H_2$  was inhaled during ischemia, infarct volume was not significantly decreased (**Fig. 5d,e**). For comparison, we tested two other compounds: edaravone (approved in Japan as an ROS scavenger for the treatment of cerebral infarction<sup>25</sup>) and FK506 (in clinical trials for cerebral infarction in the United States<sup>26</sup>).  $H_2$  was more effective than edaravone and as effective as FK506 in alleviating oxidative injury (**Fig. 5c**). These results indicate the potential of  $H_2$  for therapy.

### Inhalation of $H_2$ gas suppresses the progression of damage

At 1 week after MCA occlusion, the difference in infarct volume between untreated and  $H_2$ -treated rats increased, compared to 1d after

ischemia and reperfusion, and are one of the major causes of brain damage<sup>21,22</sup>. We produced focal ischemia in rats by occluding the middle cerebral artery (MCA) for 90 min, and then performed reperfusion for 30 min (ref. 23). In three of four conditions, rats inhaled  $H_2$  gas, mixed with nitrous oxide ( $N_2O$ ) for anesthesia, during the entire 120 min process (proportions of  $H_2$ ,  $O_2$  and  $N_2O$  (vol/vol/vol) were 1%:30%:69%, 2%:30%:68%, and 4%:30%:66%); in the fourth condition,  $H_2$  was absent, ( $H_2$ : $O_2$ : $N_2O$  (vol/vol/vol) was 0%:30%:70%). We carefully monitored physiological parameters during the experiments (Methods) and found no significant changes resulting from the inhalation of  $H_2$  (**Supplementary Table 1** online). Additionally, there was no significant influence on cerebral blood flow,

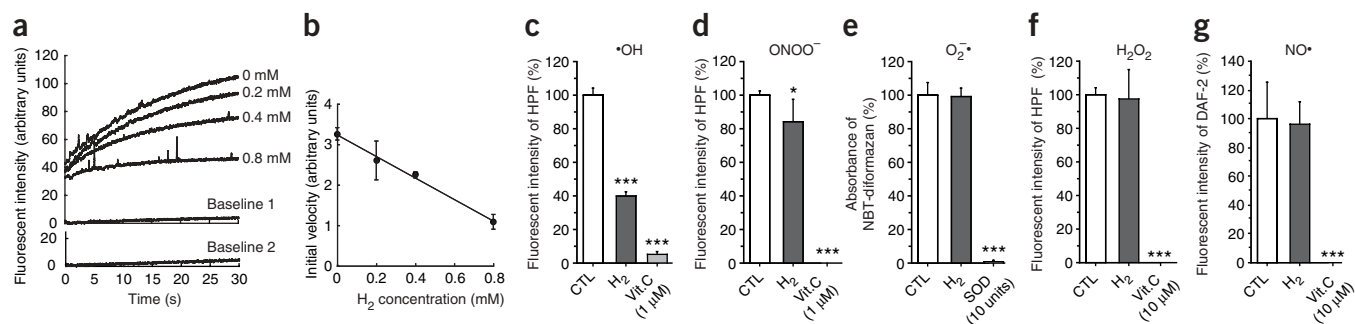


**Figure 4** Molecular hydrogen dissolved in solution scavenges hydroxyl radicals at 23 °C and pH 7.4 in cell-free systems. (a,b) The Fenton reaction, which generates hydroxyl radicals, was initiated by adding  $H_2O_2$  (to a final concentration of 5  $\mu$ M) in a closed cuvette at 23 °C with gentle stirring (**Supplementary Methods**). Levels of  $\bullet$ OH in the presence of various concentrations of  $H_2$  dissolved in the solution were assessed for HPF fluorescence. (a) Representative time course traces of HPF fluorescence at each concentration of  $H_2$ . Baselines 1 and 2 show HPF fluorescence (in the presence of 0.8 mM  $H_2$ ) in the absence of  $H_2O_2$  (baseline 1) and in the absence of ferrous perchlorate (baseline 2). (b) Mean  $\pm$  s.d. of initial rates of increase in HPF fluorescence (four independent experiments). (c–g) Levels of  $\bullet$ OH and two reactive nitrogen species (RNS:  $NO\bullet$  and peroxynitrite ( $ONOO^-$ )) remaining after incubation with 0.6 mM of  $H_2$  at 23 °C (details in the **Supplementary Methods**). Vitamin C (Vit. C) and superoxide dismutase (SOD) were used as positive controls. Signals generated in the absence of  $H_2$  (CTL) were set at 100%. Data represent mean  $\pm$  s.d. ( $n = 6$ ). \* $P < 0.05$ , \*\*\* $P < 0.001$ . NBT-diformazan: oxidized form of nitroblue tetrazolium (NBT, a detector of  $O_2\bullet^-$ ). DAF-2: diaminofluorescein-2 (a detector of  $NO\bullet$ ).

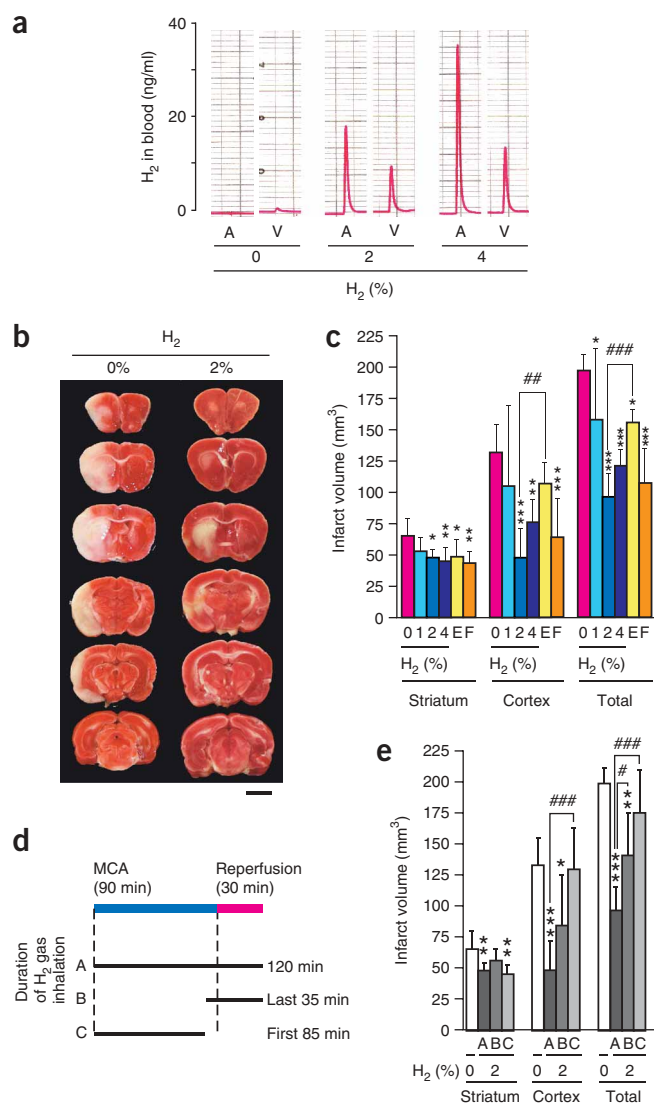


**Figure 5** Inhalation of hydrogen gas protects against ischemia-reperfusion injury. **(a)** Rats inhaled H<sub>2</sub> and 30% O<sub>2</sub> for 1 h under the anesthetics N<sub>2</sub>O and halothane. Arterial (A) and venous (V) blood were collected, and the amount of H<sub>2</sub> was examined by gas chromatography. **(b)** Rats underwent middle cerebral artery (MCA) occlusion. During the 120-min procedure, the indicated concentration of mixed gas was inhaled. One day after MCA occlusion, the forebrain was sliced into six coronal sequential sections and stained with the mitochondrial respiratory substrate TTC. Scale bar, 5 mm. **(c)** Infarct volumes of the brain were calculated in the brain slices. E and F, treatment with edaravone and FK506 ( $n = 6$ ).  $*P < 0.05$ ,  $**P < 0.01$ ,  $***P < 0.001$ , compared with 0% of H<sub>2</sub>.  $##P < 0.01$ ,  $###P < 0.001$  compared with 2% of H<sub>2</sub>. **(d)** Schematic of experiment with three different durations of hydrogen gas (2%) inhalation. **(e)** Infarct volumes of the brain for different durations of inhalation (calculated as in **c**) ( $n = 6$ ).  $*P < 0.05$ ,  $**P < 0.01$ ,  $***P < 0.001$ , compared with 0% of H<sub>2</sub>.  $#P < 0.05$ ,  $###P < 0.001$  compared with 120 min of treatment. A, B and C represent the different durations of H<sub>2</sub> gas inhalation (shown in **d**). Histograms represent mean  $\pm$  s.d.

## DISCUSSION

This study shows that molecular hydrogen can selectively reduce ROS *in vitro*. As  $\bullet\text{OH}$  and  $\text{ONOO}^-$  are much more reactive than other ROS (ref. 14), it stands to reason that H<sub>2</sub> will react with only the strongest oxidants. This is advantageous for medical procedures, as it means that the use of H<sub>2</sub> should not have serious unwanted side effects. It is likely that H<sub>2</sub> is mild enough not to disturb metabolic oxidation-reduction reactions or to disrupt ROS involved in cell signaling—unlike some antioxidant supplements with strong reductive reactivity, which increase mortality, possibly by affecting essential defensive mechanisms<sup>29</sup>.

H<sub>2</sub> has a number of advantages as a potential antioxidant: it effectively neutralizes  $\bullet\text{OH}$  in living cells, and, unlike most known antioxidants, which are unable to successfully target organelles<sup>30</sup>, it has favorable distribution characteristics: it can penetrate biomembranes and diffuse into the cytosol, mitochondria and nucleus. Despite the moderate reduction activity of H<sub>2</sub>, its rapid gaseous diffusion might make it highly effective for reducing cytotoxic radicals. Its ability to protect nuclear DNA and mitochondria suggests that it could reduce the risk of life style-related diseases and cancer.

H<sub>2</sub> markedly decreased oxidative stress and suppressed brain injury caused by ischemia and reperfusion. Inhalation of H<sub>2</sub> gas was more efficacious than a treatment currently approved for cerebral infarction and, furthermore, mitigated hepatic injury caused by ischemia and reperfusion (K. Fukuda, S.A., M.I., Y. Yamamoto, I.O. and S.O., unpublished data). This finding indicates that the beneficial effects of H<sub>2</sub> are not specific to cerebral injury but can be used for injuries in other organs.

This study suggests that H<sub>2</sub> protects cells and tissues against strong oxidative stress by scavenging  $\bullet\text{OH}$ . However, it remains possible that H<sub>2</sub> also protects from stress by directly or indirectly reducing other strong oxidant species in living cells. For instance, H<sub>2</sub> may induce cytoprotective factors; however, we found no H<sub>2</sub>-induced change in the expression of several genes involved in cytoprotection or reduction (K.N., M.I., I.O. and S.O., unpublished data). Further studies will reveal the mechanisms by which H<sub>2</sub> protects cells and tissues against oxidative stress.

Acute oxidative stress may be caused by several factors, including inflammation, intense exercise, cardiac infarction, cessation of blood flow and organ transplantation. For treatment, H<sub>2</sub> dissolved in saline could easily be delivered intravascularly. For prevention, H<sub>2</sub> saturated in water could be administered. Inhalation of H<sub>2</sub> has already been used in the prevention of decompression sickness in divers and has shown a

occlusion (Fig. 6a,b). The behavior of each rat, graded according to a neurological score<sup>27</sup>, revealed that the inhalation of H<sub>2</sub> during ischemia and reperfusion improved movement (Fig. 6c). Moreover, although body weight and body temperature of H<sub>2</sub>-untreated rats gradually declined, those in H<sub>2</sub>-treated rats eventually recovered (Fig. 6d,e). Thus H<sub>2</sub> suppressed not only the initial brain injury, but also its progressive damage.

We examined H<sub>2</sub>-mediated molecular changes at 12 h, 3 d or 7 d after occlusion, by staining brain sections with antibodies to 8-OH-G in order to assess the extent of nucleic acid oxidation (Supplementary Fig. 6 online), and with antibodies to HNE to assess lipid peroxidation (Supplementary Fig. 6). For both of these oxidative markers, staining was substantially reduced in H<sub>2</sub>-treated rats as compared to untreated rats. We also stained identical regions of the brain with antibodies to Iba1 (ref. 28) and antibodies to GFAP, which are specific to activated microglia and to astrocytes, respectively (Fig. 6f,g and Supplementary Fig. 6). We found a distinct H<sub>2</sub>-dependent decrease in the accumulation of microglia, indicative of inflammation and remodeling. Taken together, these results indicate that H<sub>2</sub> can markedly decrease oxidative stress and suppress brain injury.

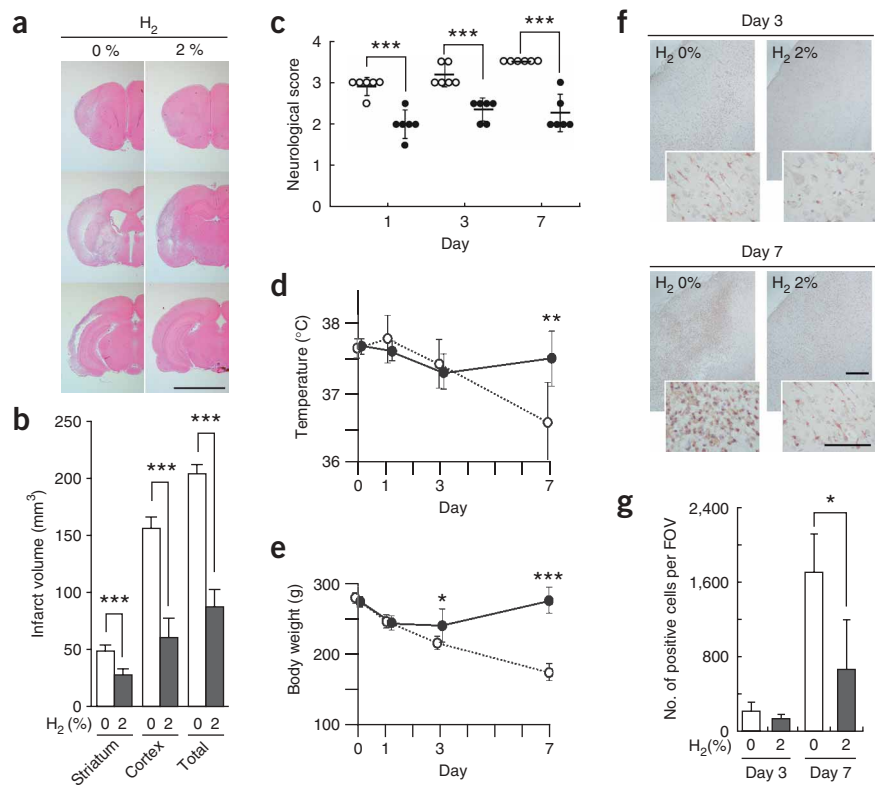


**Figure 6** Inhalation of H<sub>2</sub> gas improved brain injury after 1 week. Rats inhaled 2% of hydrogen gas during the 120-min ischemia and reperfusion procedure and were maintained for 1, 3 or 7 d. **(a)** One week after MCA occlusion, the brains were sliced and stained with hematoxylin and eosin. Three representative slices are shown. Scale bar, 5 mm. **(b)** Infarct volumes (light-pink regions in **a**) were calculated ( $n = 6$ ).  $***P < 0.001$ . **(c)** Neurological scores were graded on a scale of 0 to 5, as described previously<sup>27</sup>; score 0, no neurological deficit; 1, failure to fully extend the right forepaw; 2, circling to the right; 3, falling to the right; 4, unable to walk spontaneously; and 5, dead. When a rat's neurological score was judged to be between 1 and 2, 2 and 3, or 3 and 4, the score was set at 1.5, 2.5 and 3.5, respectively. Closed and open circles represent treatment with or without H<sub>2</sub> ( $n = 6$ ).  $***P < 0.001$ . **(d,e)** Body weights and temperature were monitored with (closed circles) or without (open circles) inhalation of 2% hydrogen gas ( $n = 6$ ).  $*P < 0.05$ ,  $**P < 0.01$ ,  $***P < 0.001$ . **(f)** On days 3 or 7 after MCA occlusion, coronal 6- $\mu$ m sections from the ischemic core area in the temporal cortex were stained with antibody to Iba1 (a microglial marker). Scale bar, 200  $\mu$ m (100  $\mu$ m in the inset). **(g)** Cells positive for the Iba1 antibody<sup>28</sup>, per field of view (FOV), were counted in the ischemic core area, as indicated in **f** ( $n = 6$ ).  $*P < 0.05$ . Data represent mean  $\pm$  s.d.

good safety profile<sup>31</sup>. Notably, H<sub>2</sub> has no risk of flammability or explosion at a concentration of less than 4.7% in air. We propose that H<sub>2</sub>, one of the most well-known molecules, could be widely used in medical applications as a safe and effective antioxidant with minimal side effects.

## METHODS

**Hydrogen and oxygen measurements.** We measured molecular hydrogen (H<sub>2</sub>) and oxygen (dioxigen, O<sub>2</sub>) dissolved in solution by using a hydrogen electrode (ABLE) and an oxygen electrode (Strathkelvin Instruments), respectively. We determined hydrogen gas concentration by gas chromatography (Teramecs). For measuring H<sub>2</sub> levels in blood, we pretreated rats with heparin to avoid blood clotting, collected arterial and venous blood (5 ml each) in test tubes, and then immediately injected the blood samples into closed aluminum bags containing 30 ml of air. After complete transfer of the H<sub>2</sub> gas from the blood to the air in the closed bag, we subjected 20 ml of the air to gas chromatography using standard H<sub>2</sub> gas, in order to quantify the amount of H<sub>2</sub>.

**Hydrogen treatment of cultured cells.** Over a 2-h period, we dissolved H<sub>2</sub> beyond saturation levels into DMEM medium under 0.4 MPa pressure. We dissolved O<sub>2</sub> into a second medium by bubbling O<sub>2</sub> gas at the saturated level (42.5 mg/l), and CO<sub>2</sub> into a third medium by bubbling CO<sub>2</sub> gas. All three media were maintained at atmospheric pressure. We then combined the three media (H<sub>2</sub> medium:O<sub>2</sub> medium:CO<sub>2</sub> medium) in the proportion 75%:20%:5% (vol/vol/vol) and added fetal bovine serum (FBS) to achieve a final concentration of 1%. For culture, we put the combined medium into a culture flask and immediately examined H<sub>2</sub> or O<sub>2</sub> concentration with an H<sub>2</sub> or O<sub>2</sub> electrode. Then we filled the culture flask with mixed gas consisting of 75% H<sub>2</sub>, 20% O<sub>2</sub> and 5% CO<sub>2</sub> (vol/vol/vol) and cultured cells in the closed culture flask. We prepared degassed medium lacking H<sub>2</sub> by stirring the medium, which had been saturated with H<sub>2</sub>, in an open vessel for 4 h, and checked the concentration of H<sub>2</sub> with a hydrogen electrode. In the experiments on the dose dependence of H<sub>2</sub> (results shown in Fig. 2f), we diluted the combined medium with a fourth medium containing 1% FBS equilibrated with air containing 5% CO<sub>2</sub>, in order

to obtain the desired concentration of H<sub>2</sub>; we then filled the culture flasks with the mixed gas diluted with air containing 5% CO<sub>2</sub>.

**Induction of oxidative stress by antimycin A and menadione.** We maintained PC12 cells at 37 °C in DMEM medium containing 1% FBS with or without 0.6 mM H<sub>2</sub> in a closed flask filled with mixed gases as described above. We treated the cells with menadione or antimycin A, which inhibit complex I or complex III, respectively, of the mitochondrial electron transport chain, and thus produce O<sub>2</sub><sup>•</sup> (by accelerating the leakage of electrons). After exposure to antimycin A for 24 h, we assessed cell survival by manually counting the cells double-stained with 1  $\mu$ M propidium iodide (dead cells labeled pink) and 5  $\mu$ M Hoechst 33342 (dead and living cells labeled blue) under a fluorescent microscope. To examine the protective effect by H<sub>2</sub> on mitochondria, we pretreated cells with 4.5 g/l 2-deoxy-D-glucose (an inhibitor of glycolysis) and 1 mM pyruvate (a substrate of oxidative phosphorylation) for 30 min, exposed them to antimycin A with or without 0.6 mM H<sub>2</sub> and then quantified cellular ATP levels using a cellular ATP measurement kit (TOYO B-Net).

**Cerebral infarction model.** Animal protocols were approved by the Animal Care and Use Committee of Nippon Medical School. We anesthetized male Sprague-Dawley rats (body weight: 250–300 g) with halothane (4% for induction, 1% for maintenance) in a mixture of nitrous oxide and oxygen (70%:30%, vol/vol). We maintained temperature (37.5  $\pm$  0.5 °C) using a thermostatically controlled heating blanket connected to a thermometer probe in the rectum, and, at the same time, monitored physiological parameters (using a cannula in the tail artery), including blood gases (pCO<sub>2</sub> and pO<sub>2</sub>), pH, glucose level and blood pressure. We attempted to maintain constant levels of pH and pO<sub>2</sub> by regulating the amount of halothane and the N<sub>2</sub>O:O<sub>2</sub> ratio. We produced focal ischemia by performing intraluminal occlusion of the left middle cerebral artery (MCA), using a nylon monofilament with a rounded tip and a distal silicon rubber cylinder as previously described<sup>23</sup>. The rats underwent MCA occlusion for 90 min and then reperfusion for 30 min; they inhaled H<sub>2</sub> gas during the entire process except in the experiments corresponding to Figure 5d,e. We treated rats with edaravone and FK506 using the most effective concentrations (refs. 25, 23 and Fig. 5c). After the rats recovered from anesthesia, they were maintained at 23 °C.

At 24 h after MCA occlusion, we removed brains under anesthesia and sliced them into six coronal sequential sections (2 mm thick). We stained the sections with 2,3,5-triphenyltetrazolium chloride (TTC) (3%), and then measured infarct and noninfarct areas using an optical dissector image analysis system (Mac SCOPE, Mitsuya Shoji). We outlined the border between infarct and noninfarct tissues, and obtained the area of infarction by subtracting the nonlesioned area of the ipsilateral hemisphere from that of the contralateral side. We calculated the volume of infarction as infarct area  $\times$  thickness. At 12 h, 3 d or 7 d after MCA occlusion, we quickly removed brains under anesthesia, and fixed them with 10% formalin. We sliced paraffin-embedded brains into a series of 6- $\mu$ m sections, and stained sections with hematoxylin and eosin (H&E). We then quantified the pink areas with a graphic analyzer system (Mac Scope). For immunostaining, we stained the sections with antibodies by using VECTASTAIN ABC reagents according to the supplier's instructions.

**Statistical analysis.** We used StatView software (SAS Institute) for the statistical analyses. For single comparisons, we performed an unpaired two-tailed Student's *t*-test; for multiple comparisons, we used an analysis of variance (ANOVA) followed by Fisher's exact test. We performed experiments for quantification in a blinded fashion.

*Note: Supplementary information is available on the Nature Medicine website.*

#### ACKNOWLEDGMENTS

This work was supported by grants to S.O. from the Ministry of Health, Labor and Welfare (H17-Chouju-009, longevity science; and 17A-10, nervous and mental disorders) and the Ministry of Education, Culture, Sports, Science and Technology (16390257).

#### AUTHOR CONTRIBUTIONS

S.O. conceived the experiments. S.O., I.O., K.K. and Y.K. designed the experiments. I.O., S.A. and S.O. performed data analysis. I.O., M.I., K.T., M.W., K.N., K.Y., S.A. and S.O. performed the experiments. S.O. and I.O. wrote the paper.

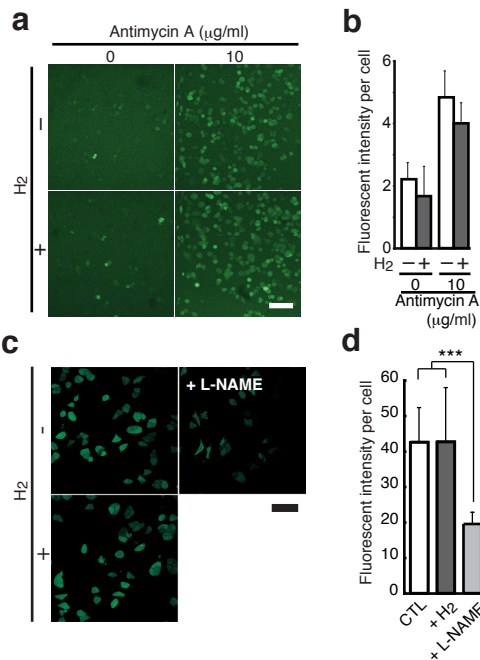
#### COMPETING INTERESTS STATEMENT

The authors declare no competing financial interests.

Published online at <http://www.nature.com/naturemedicine>

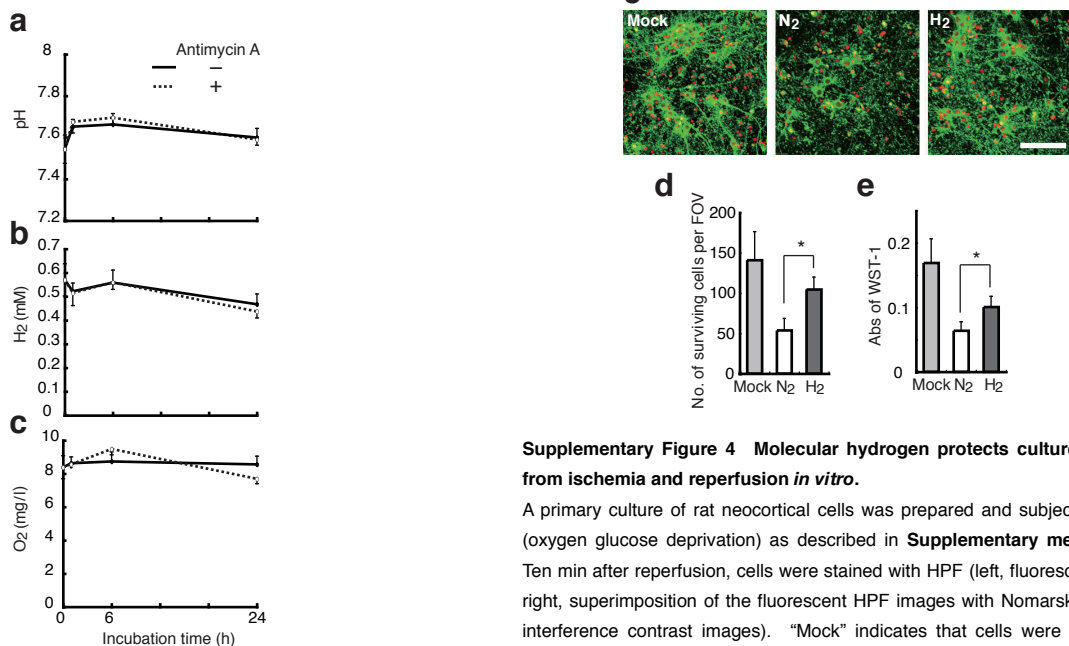
Reprints and permissions information is available online at <http://npg.nature.com/reprintsandpermissions>

- Wallace, D.C. A mitochondrial paradigm of metabolic and degenerative diseases, aging, and cancer: a dawn for evolutionary medicine. *Annu. Rev. Genet.* **39**, 359–407 (2005).
- Reddy, P.H. Amyloid precursor protein-mediated free radicals and oxidative damage: implications for the development and progression of Alzheimer's disease. *J. Neurochem.* **96**, 1–13 (2006).
- Ohta, S. A multi-functional organelle mitochondrion is involved in cell death, proliferation and disease. *Curr. Med. Chem.* **10**, 2485–2494 (2003).
- Wright, E., Jr., Scism-Bacon, J.L. & Glass, L.C. Oxidative stress in type 2 diabetes: the role of fasting and postprandial glycaemia. *Int. J. Clin. Pract.* **60**, 308–314 (2006).
- Winterbourn, C.C. Biological reactivity and biomarkers of the neutrophil oxidant, hypochlorous acid. *Toxicology* **181**, 223–227 (2002).
- Chinopoulos, C. & Adam-Vizi, V. Calcium, mitochondria and oxidative stress in neuronal pathology. Novel aspects of an enduring theme. *FEBS J.* **273**, 433–450 (2006).
- Sauer, H., Wartenberg, M. & Hescheler, J. Reactive oxygen species as intracellular messengers during cell growth and differentiation. *Cell. Physiol. Biochem.* **11**, 173–186 (2001).
- Turrens, J.F. Mitochondrial formation of reactive oxygen species. *J. Physiol. (Lond.)* **552**, 335–344 (2003).
- Sheu, S.S., Nauduri, D. & Anders, M.W. Targeting antioxidants to mitochondria: a new therapeutic direction. *Biochim. Biophys. Acta* **1762**, 256–265 (2006).
- Liu, H., Colavitti, R., Rovira, I.I. & Finkel, T. Redox-dependent transcriptional regulation. *Circ. Res.* **97**, 967–974 (2005).
- Murad, F. Discovery of some of the biological effects of nitric oxide and its role in cell signaling. *Biosci. Rep.* **24**, 452–474 (2004).
- Buxton, G.V., Greenstock, C.L., Helman, W.P. & Ross, A.B. Critical review of rate constants for reactions of hydrated electrons, hydrogen atoms and hydroxyl radicals ( $\bullet\text{OH}/\text{HO}\bullet$ ) in aqueous solution. *J. Phys. Chem. Ref. Data* **17**, 513–886 (1988).
- Ohsawa, I., Nishimaki, K., Yasuda, C., Kamino, K. & Ohta, S. Deficiency in a mitochondrial aldehyde dehydrogenase increases vulnerability to oxidative stress in PC12 cells. *J. Neurochem.* **84**, 1110–1117 (2003).
- Setsubukinai, K., Urano, Y., Kakinuma, K., Majima, H.J. & Nagano, T. Development of novel fluorescence probes that can reliably detect reactive oxygen species and distinguish specific species. *J. Biol. Chem.* **278**, 3170–3175 (2003).
- Tomizawa, S. *et al.* The detection and quantification of highly reactive oxygen species using the novel HPF fluorescence probe in a rat model of focal cerebral ischemia. *Neurosci. Res.* **53**, 304–313 (2005).
- Kamiya, H. Mutagenicities of 8-hydroxyguanine and 2-hydroxyadenine produced by reactive oxygen species. *Biol. Pharm. Bull.* **27**, 475–479 (2004).
- Petersen, D.R. & Doorn, J.A. Reactions of 4-hydroxynonenal with proteins and cellular targets. *Free Radic. Biol. Med.* **37**, 937–945 (2004).
- Falick, A.M., Mahan, B.H. & Myers, R.J. Paramagnetic resonance spectrum of the  $^1\Delta_g$  oxygen molecule. *J. Chem. Phys.* **42**, 1837–1838 (1965).
- Asoh, S. *et al.* Protection against ischemic brain injury by protein therapeutics. *Proc. Natl. Acad. Sci. USA* **99**, 17107–17112 (2002).
- Halestrap, A.P. Calcium, mitochondria and reperfusion injury: a pore way to die. *Biochem. Soc. Trans.* **34**, 232–237 (2006).
- Lipton, P. Ischemic cell death in brain neurons. *Physiol. Rev.* **79**, 1431–1568 (1999).
- Ferrari, R. *et al.* Oxidative stress during myocardial ischaemia and heart failure. *Curr. Pharm. Des.* **10**, 1699–1711 (2004).
- Nito, C., Kamiya, T., Ueda, M., Arai, T. & Katayama, Y. Mild hypothermia enhances the neuroprotective effects of FK506 and expands its therapeutic window following transient focal ischemia in rats. *Brain Res.* **1008**, 179–185 (2004).
- Takada, J. *et al.* Adenovirus-mediated gene transfer to ischemic brain is augmented in aged rats. *Exp. Gerontol.* **38**, 423–429 (2003).
- Zhang, N. *et al.* Edaravone reduces early accumulation of oxidative products and sequential inflammatory responses after transient focal ischemia in mice brain. *Stroke* **36**, 2220–2225 (2005).
- Labiche, L.A. & Grotta, J.C. Clinical trials for cytoprotection in stroke. *NeuroRx* **1**, 46–70 (2004).
- Murakami, K. *et al.* Mitochondrial susceptibility to oxidative stress exacerbates cerebral infarction that follows permanent focal cerebral ischemia in mutant mice with manganese superoxide dismutase deficiency. *J. Neurosci.* **18**, 205–213 (1998).
- Ito, D. *et al.* Microglia-specific localisation of a novel calcium binding protein, Iba1. *Brain Res. Mol. Brain Res.* **57**, 1–9 (1998).
- Bjelakovic, G., Nikolova, D., Gluud, L.L., Simonetti, R.G. & Gluud, C. Mortality in randomized trials of antioxidant supplements for primary and secondary prevention: systematic review and meta-analysis. *J. Am. Med. Assoc.* **297**, 842–857 (2007).
- James, A.M., Cocheme, H.M. & Murphy, M.P. Mitochondria-targeted redox probes as tools in the study of oxidative damage and ageing. *Mech. Ageing Dev.* **126**, 982–986 (2005).
- Fontanari, P. *et al.* Changes in maximal performance of inspiratory and skeletal muscles during and after the 7.1-MPa Hydra 10 record human dive. *Eur. J. Appl. Physiol.* **81**, 325–328 (2000).



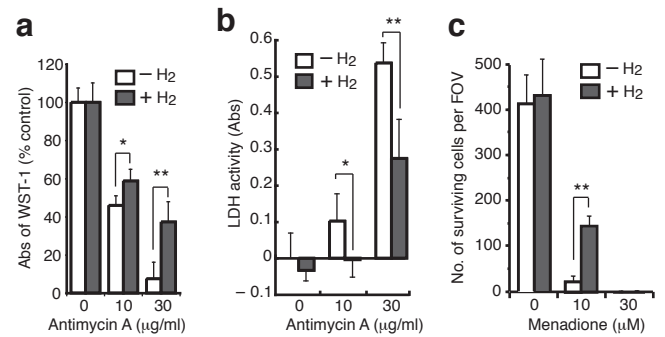
**Supplementary Figure 1 Molecular hydrogen dissolved in culture medium does not reduce cellular hydrogen peroxide and nitric oxide.**

(a) PC12 cells were held in medium with or without 0.6 mM  $\text{H}_2$ , and antimycin A (10  $\mu\text{g/ml}$ ) was added to the medium to induce  $\text{O}_2^{\cdot-}$ , which was rapidly converted into  $\text{H}_2\text{O}_2$ . Representative laser-scanning confocal images of the fluorescence of  $\text{H}_2\text{O}_2$  marker 2',7'-dichlorodihydrofluorescein ( $\text{H}_2\text{DCF}$ ) were taken 1 h after the addition of antimycin A. Scale bar: 100  $\mu\text{m}$ . (b) DCF fluorescence in cells treated with antimycin A in the presence or absence of 0.6 mM  $\text{H}_2$  was quantified from 100 cells from each independent experiment using NIH Image software (mean  $\pm$  SD, *n* = 4). (c, d) Cellular  $\text{NO}^{\cdot}$  was detected with a cellular  $\text{NO}^{\cdot}$ -specific fluorescent probe, DAF-2 DA (diaminofluorescein-2 diacetate, purchased from Daiichi Pure Chemicals Co.) by laser-scanning confocal microscopy using excitation and emission filters of 488 and 510 nm, respectively. As a negative control, an inhibitor of NOS (L-NAME:  $\text{N}^G$ -Nitro-L-arginine methyl ester, purchased from Sigma) was added so as not to generate  $\text{NO}^{\cdot}$ . Scale bar: 50  $\mu\text{m}$ . (d) DAF-2 DA fluorescence was quantified as described in (b) (mean  $\pm$  SD, *n* = 5). \*\*\**P* < 0.001.



**Supplementary Figure 2 pH,  $\text{H}_2$  and  $\text{O}_2$  maintain constant in culture medium in a closed flask filled with a mixed gas.**

DMEM culture medium with dissolved  $\text{H}_2$  and  $\text{O}_2$  was prepared as described in **Methods**. PC12 cells ( $5 \times 10^5$ ) were cultured in medium with or without antimycin A (10  $\mu\text{g/ml}$ ) in a closed culture flask (25  $\text{cm}^2$ ) filled with a mixed gas composed of 75% of  $\text{H}_2$ , 20% of  $\text{O}_2$  and 5% of  $\text{CO}_2$ . At the indicated time, pH,  $\text{H}_2$  or  $\text{O}_2$  in the medium was monitored with a pH meter,  $\text{H}_2$  or  $\text{O}_2$  electrode. One flask was used for one measurement. Data show the mean  $\pm$  SD (*n* = 4).

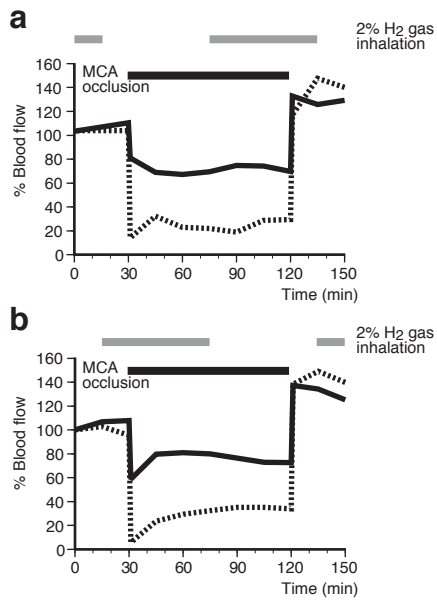


**Supplementary Figure 3 Several methods confirm protection of cells by  $\text{H}_2$  against oxidative stress.**

PC12 cells incubated in the presence of or absence of 0.6 mM  $\text{H}_2$  were treated with the indicated concentration of antimycin A (a, b) or menadione (c), and maintained with each  $\text{H}_2$  concentration for 24 h as described in **Methods**. (a) As another method, a modified MTT assay (WST-1 assay) was applied to the cell system according to a Cell Counting Kit (purchased from Wako) to ensure the protective effect by  $\text{H}_2$  against oxidative stress (mean  $\pm$  SD, *n* = 4). \**P* < 0.05, \*\**P* < 0.01. (b) Lactate dehydrogenase (LDH) activities were measured to estimate cellular LDH leakage from damaged cells according to an LDH-Cytotoxic Test kit (Wako). LDH activity in medium of antimycin A- and  $\text{H}_2$ -untreated cells was taken as the background (mean  $\pm$  SD, *n* = 4). \**P* < 0.05, \*\**P* < 0.01. (c) Instead of antimycin A, menadione was used to induce oxidative stress for 24 h and living cells were enumerated as described in **Fig. 2f** (mean  $\pm$  SD, *n* = 4). \*\**P* < 0.01.

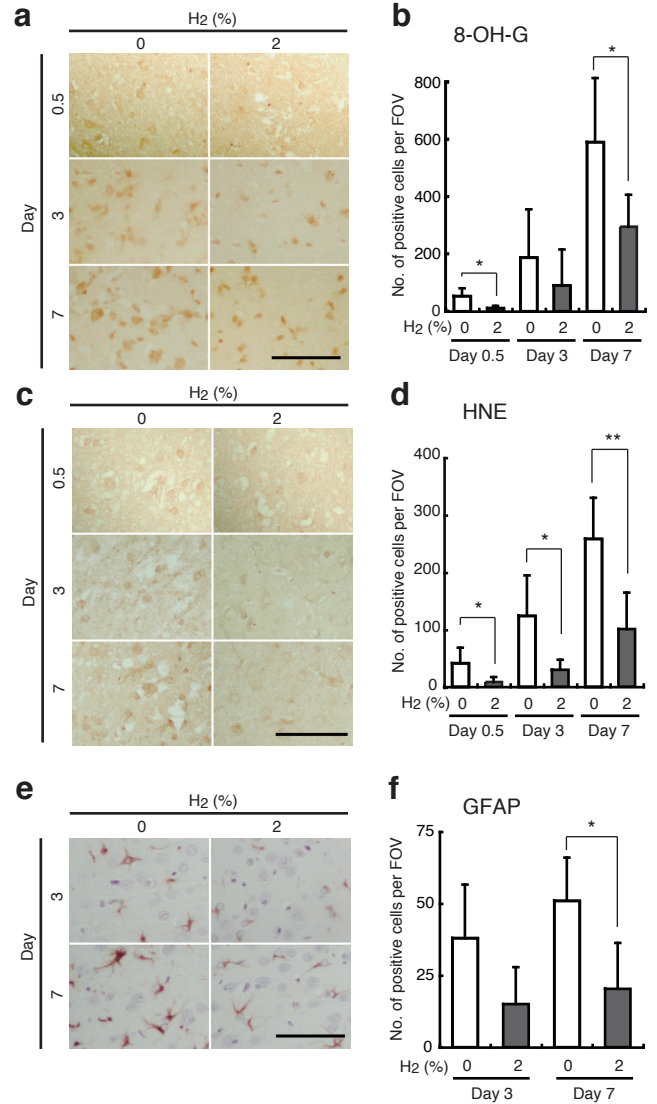
**Supplementary Figure 4 Molecular hydrogen protects cultured neurons from ischemia and reperfusion *in vitro*.**

A primary culture of rat neocortical cells was prepared and subjected to OGD (oxygen glucose deprivation) as described in **Supplementary methods**. (a) Ten min after reperfusion, cells were stained with HPF (left, fluorescent images; right, superimposition of the fluorescent HPF images with Nomarski differential interference contrast images). "Mock" indicates that cells were treated with DMEM medium containing glucose and oxygen instead of being subjected to OGD. Scale bar: 100  $\mu\text{m}$ . (b) The average fluorescent intensity of HPF was measured in 100 cells (mean  $\pm$  SD, *n* = 4). \**P* < 0.05. (c) Twenty hours after OGD, surviving neurons were fixed and immunostained with the neuron-specific antibody to TUJ-1 (green) and with PI (red). Scale bar: 100  $\mu\text{m}$ . (d) Dead cells were washed out in the staining procedure and living cells were enumerated under a fluorescent microscope in four fields of view (FOV) per well (mean  $\pm$  SD, *n* = 4). \**P* < 0.05. (e) Twenty hours after OGD, viability in a well was estimated by a modified MTT viability assay according to a Cell Counting Kit (WST-1 assay) (mean  $\pm$  SD, *n* = 4). \**P* < 0.05.



**Supplementary Figure 5 Cerebral blood flow is not influenced by H<sub>2</sub> inhalation.**

Middle cerebral artery occlusion was produced as described in **Methods**. Cerebral blood flow was measured by laser Doppler flowmetry using an ALF21 (ADVANCE Co.) at 2 mm lateral to the bregma for penumbra (solid line) and 5 mm lateral to the bregma for ischemic core (dotted line). Periods of 2% H<sub>2</sub> inhalation and middle cerebral artery (MCA) occlusion are shown by grey and solid thick lines, respectively.



**Supplementary Figure 6 The brain after induction of ischemia reperfusion injury with or without H<sub>2</sub> treatment was immunostained.**

Twelve h (0.5 d), 3 or 7 d after MCA occlusion, the brains were fixed and embedded in paraffin. Coronal 6- $\mu$ m-sections were stained with antibody to 8-OH-G in the ischemic penumbra area in the temporal cortex (**a**), with antibody to HNE in the ischemic penumbra area in the temporal cortex (**c**), and with antibody to GFAP in the ischemic penumbra area in the occipital cortex (**e**). Scale bar: 100  $\mu$ m. Positive cells with antibodies to 8-OH-G (**b**), HNE (**d**) and GFAP (**f**) per field of view (FOV) were counted in exactly the same regions in a blinded manner (mean  $\pm$  SD,  $n = 6$ ). \* $P < 0.05$ , \*\* $P < 0.01$ .

## Supplementary methods

**Detection of ROS by fluorescent indicators.** We treated PC12 cells with 10  $\mu\text{M}$  of 5-(and-6)-chloromethyl-2',7'-dichlorodihydrofluorescein diacetate, acetyl ester (CM-H<sub>2</sub>DCFDA) (purchased from Molecular Probes), 5  $\mu\text{M}$  diaminofluorescein-2 diacetate (DAF-2 DA) (purchased from Daiichi Pure Chemicals Co.), or 5  $\mu\text{M}$  of 2-[6-(4'-hydroxy)phenoxy-3*H*-xanthen-3-on-9-yl]benzoate (HPF) (Daiichi Pure Chemicals Co.) for 30 min to detect cellular H<sub>2</sub>O<sub>2</sub>, NO• or •OH, respectively. We took fluorescent images with a laser-scanning confocal microscope (Olympus FV300) using excitation and emission filters of 488 nm and 510 nm, respectively. HPF can be specifically oxidized by •OH, peroxynitrite (ONOO<sup>-</sup>) and lipid peroxides, but neither H<sub>2</sub>O<sub>2</sub>, NO• nor O<sub>2</sub><sup>-•</sup> (ref. 14). For the detection of cellular O<sub>2</sub><sup>-•</sup>, we used 0.5  $\mu\text{M}$  MitoSOX (purchased from Molecular Probes), and took images using excitation and emission filters of 543 nm and 565 nm, respectively. Fluorescent signals were quantified from 100 cells of each experiment using US National Institutes of Health Image software.

**Staining of mitochondria.** For staining of mitochondria, we co-stained with MitoTracker Green (MTGreen) (1  $\mu\text{M}$ ; Molecular Probes) and tetramethylrhodamine methyl ester (TMRM) (100 nM; Molecular Probes). Fluorescence from MTGreen is independent of the membrane potential, whereas that from TMRM is sensitive to the membrane potential. MTGreen and TMRM were detected using excitation at 488 and 543 nm, and emission filters of 510 and 565 nm, respectively.

**Immunostaining.** We purchased antibodies against HNE and 8-OH-G from Nikken Seil Co, and antibodies against TUJ-1 and GFAP from COVANCE and ThermoFisher, respectively. We used BODIPY FL goat anti-mouse IgG (Molecular Probe) as a secondary antibody and visualized signals with a laser-scanning confocal microscope. Fluorescence signals in response to 8-OH-G and HNE were quantified with NIH Image software.

**Intracellular Fenton reaction.** We preincubated PC12 cells with 1 mM CuSO<sub>4</sub> for 30 min in medium containing 1% FCS, washed once with phosphate-buffered saline (PBS) containing CaCl<sub>2</sub> (0.1 g/l), MgCl<sub>2</sub>·6H<sub>2</sub>O (0.1 g/l), glucose (1g/l) and sodium pyruvate (0.036 g/l) (pH 7.2), and then exposed to the indicated concentration of ascorbate (vitamin C) for 1 h in phosphate-buffered saline as described above. As negative controls, CuSO<sub>4</sub> or ascorbate was omitted. Note that Cu<sup>+2</sup> is reduced by ascorbate to Cu<sup>+</sup>, which catalyzes the Fenton reaction to produce •OH from H<sub>2</sub>O<sub>2</sub> that is being spontaneously produced in the cells.

**Electron spin resonance measurement.** We used 5,5-dimethyl-1-pyrroline *N*-oxide (DMPO) as a free radical trapper, and detected electron spin resonance (ESR) signals with a KEYCOM ESR spectrometer type ESR-X01. As a standard of the reactant of •OH with DMPO, we produced •OH by the Fenton reaction in the mixture of 0.1 mM H<sub>2</sub>O<sub>2</sub> and 1 mM FeCl<sub>2</sub> in the presence of 0.1 mM DMPO and

subjected the whole solution to ESR measurement. For the measurements, we normalized the sensitivity of each experiment with the strength of the internal ESR signal derived from Mn<sup>2+</sup>. To obtain a spectrum, ESR was scanned for 2 min, accumulated 10 times, and all signals were averaged.

For H<sub>2</sub> treatment, we prepared media containing 0.6 mM H<sub>2</sub> and 8.5 mg/l O<sub>2</sub>, and filled a closed culture flask with 75% H<sub>2</sub>, 20% O<sub>2</sub> and 5% CO<sub>2</sub> gases. We pretreated PC12 cells (2 × 10<sup>6</sup> cells in a 25 cm<sup>2</sup> flask) with 0.1 M DMPO and 2 mM CuSO<sub>4</sub> in DMEM containing 1% FCS for 30 min at 37 °C in the presence or absence of 0.6 mM H<sub>2</sub>. After the removal of this medium, we exposed the cells to 0.2 mM ascorbate and 0.1 mM H<sub>2</sub>O<sub>2</sub> in 0.3 ml of PBS in the presence or absence of 0.6 mM H<sub>2</sub> for 5 min at room temperature to produce •OH by the Fenton reaction, and scraped the cells into a flat cuvette for ESR measurement. In the other method, we preincubated PC12 cells (2 × 10<sup>6</sup> cells in a 25 cm<sup>2</sup> flask) in 0.3 ml of PBS containing 0.1 M DMPO and 30  $\mu\text{g/ml}$  antimycin A for 7 min at room temperature in the presence or absence of 0.6 mM H<sub>2</sub>, and then scraped the cells into a flat cuvette for ESR measurement. A differential spectrum was obtained by digitally subtracting one spectrum from the other to visualize the signals decreased by H<sub>2</sub> treatment.

**Primary culture.** We prepared primary cultures of neocortical neurons from 16-day rat embryos by the method described previously<sup>19</sup>. In brief, neocortical tissues were cleaned of meninges, minced, and treated with a protease cocktail (SUMILON). After mechanical dissociation by pipetting, we resuspended cells in nerve-cell culture medium (SUMILON), and then plated onto poly-L-lysine-coated plates at a density of 5 × 10<sup>4</sup> cells / cm<sup>2</sup>, changed to Neurobasal Medium (Invitrogen) with B-27 (Invitrogen) once every three days and then used neurons at day 11. One day before OGD, we changed the medium to Neurobasal Medium with B-27 minus AO (Invitrogen), and confirmed neuronal identity by immunostaining with antibodies to neuron marker TUJ-1, and astrocyte marker GFAP. We used preparations only containing over 90% neurons for experiments.

**Oxygen-glucose deprivation.** To initiate OGD, we replaced the culture medium with a glucose-deficient DMEM from which O<sub>2</sub> had been removed by bubbling in a mixed gas of either N<sub>2</sub> (95%):CO<sub>2</sub> (5%) or H<sub>2</sub> (95%):CO<sub>2</sub> (5%) and maintained the culture for 60 min at 30 °C under an atmosphere of either N<sub>2</sub> (95%):CO<sub>2</sub> (5%) or H<sub>2</sub> (95%):CO<sub>2</sub> (5%). Treatment was terminated by exchanging the experimental medium with stocked culture medium and further incubation at 37 °C with air including 5% CO<sub>2</sub>.

**Reaction of H<sub>2</sub> in cell-free systems.** We performed fluorescence spectroscopic studies with a Shimadzu RF-5300PC. For solution studies, we dissolved H<sub>2</sub> in water beyond the saturated level under 0.4 MPa of hydrogen pressure for 2 h and then used it under atmospheric pressure. We determined H<sub>2</sub> concentrations with a hydrogen electrode in each experiment.

To detect the reaction of H<sub>2</sub> with the oxidized form of cytochrome *c*, FAD, or NAD<sup>+</sup>, we incubated solutions containing 10  $\mu\text{M}$

cytochrome *c*, 1 mM FAD or 1 mM NAD<sup>+</sup> with or without 0.8 mM H<sub>2</sub> in a closed cuvette at 23 °C for 30 min, and observed no reaction by absorbance at 415, 400 and 340 nm, respectively.

We monitored the reactivity of H<sub>2</sub> with various ROS by HPF, DAF-2, or nitroblue tetrazolium (NBT). We measured fluorescent signals of HPF and DAF-2 at 515 nm with excitation at 490 and 495 nm, respectively, and the reduction of NBT to NBT-diformazan by absorbance at 550 nm.

To detect the reaction of H<sub>2</sub> with •OH, we mixed hydrogen solution, phosphate buffer (10 mM at pH 7.4), ferrous perchlorate (0.1 mM), and HPF (0.4 μM). We initiated the Fenton reaction by adding H<sub>2</sub>O<sub>2</sub> to 5 μM in a closed cuvette at 23 °C with gentle stirring and monitored fluorescence for 30 s.

To detect the reaction of H<sub>2</sub> with O<sub>2</sub><sup>-•</sup>, we mixed solutions containing xanthine and NBT (supplied by TREVIGEN) with or without 0.8 mM H<sub>2</sub> in a closed cuvette, initiated the reaction by adding xanthine oxidase at 23 °C and monitored for 5 min.

To detect the reaction of H<sub>2</sub> with H<sub>2</sub>O<sub>2</sub>, we incubated solutions including phosphate buffer (10 mM at pH 7.4) and H<sub>2</sub>O<sub>2</sub> (10 μM) with or without H<sub>2</sub> (0.8 mM) in a closed glass tube at 23 °C for 30 min. We converted the remaining H<sub>2</sub>O<sub>2</sub> to •OH by 0.2 μM horseradish peroxidase and then incubated with 10 μM HPF for 5 min.

To detect the reaction of H<sub>2</sub> with NO•, we incubated solutions containing phosphate buffer (10 mM at pH 7.4) and 1-hydroxy-2-oxo-3-(*N*-methyl-3-aminopropyl)-3-methyl-1-triazene (NOC7, 0.1 μM, purchased from Dojin Chemicals Co.) with or without 0.8 mM H<sub>2</sub> in a closed cuvette at 23 °C for 30 min, and monitored the remaining NO• by incubation with 5 μM DAF-2 for 10 min.

To detect the reaction of H<sub>2</sub> with peroxynitrite (ONOO<sup>-</sup>), we diluted a stock solution of 1 μM ONOO<sup>-</sup> in alkali 200-fold into 10 mM phosphate buffer with 0.4 μM HPF in the presence or absence of 0.8 mM H<sub>2</sub>, and then examined HPF signals after 23 °C for 1 min.

**Supplementary Table 1**

Physiological parameters during cerebral ischemia reperfusion

preischemia							ischemia						
0% H <sub>2</sub>							0% H <sub>2</sub>						
No.	temp. (°C)	pH	pCO <sub>2</sub>	pO <sub>2</sub>	glucose (mg/dl)	pressure (mmHg)	No.	temp. (°C)	pH	pCO <sub>2</sub>	pO <sub>2</sub>	glucose (mg/dl)	pressure (mmHg)
1	37.4	7.47	39	107	120	110	1	37.4	7.42	44	89	130	145
2	37.5	7.39	51	113	114	95	2	37.1	7.40	51	98	117	120
3	37.5	7.47	43	109	119	108	3	37.4	7.44	47	115	115	130
4	37.4	7.46	43	134	120	110	4	37.0	7.42	48	119	117	150
5	37.1	7.44	40	109	103	110	5	37.5	7.42	42	113	105	150
6	37.2	7.45	39	125	110	120	6	37.5	7.44	41	112	105	153
Average	37.4	7.45	43	116	114	109	Average	37.3	7.42	46	108	115	141
S.D.	0.2	0.03	5	11	7	8	S.D.	0.2	0.02	4	12	9	13
2% H <sub>2</sub>							2% H <sub>2</sub>						
1	37.1	7.45	46	130	109	105	1	37.3	7.41	48	111	120	120
2	37.4	7.44	50	118	104	87	2	37.6	7.43	43	99	97	135
3	37.7	7.40	46	105	114	103	3	37.8	7.42	45	104	100	150
4	36.9	7.45	47	121	107	100	4	37.0	7.39	52	97	105	150
5	37.5	7.46	41	120	109	100	5	37.3	7.41	45	109	107	145
6	37.0	7.46	45	114	107	115	6	37.5	7.42	47	108	113	160
Average	37.3	7.44	46	118	108	102	Average	37.4	7.41	47	105	107	143
S.D.	0.3	0.02	3	8	3	9	S.D.	0.3	0.01	3	6	8	14
4% H <sub>2</sub>							4% H <sub>2</sub>						
1	37.6	7.48	36	118	113	120	1	37.0	7.40	48	110	105	145
2	37.2	7.45	40	134	96	112	2	36.8	7.40	46	107	94	120
3	37.6	7.46	43	119	90	125	3	37.0	7.41	47	83	91	130
4	36.7	7.46	39	128	103	120	4	37.6	7.43	43	111	97	145
5	36.8	7.43	45	111	97	120	5	37.4	7.45	44	105	100	140
6	37.5	7.49	34	127	103	100	6	37.4	7.44	46	110	105	150
Average	37.2	7.46	40	123	100	116	Average	37.2	7.42	46	104	99	138
S.D.	0.4	0.02	4	8	8	9	S.D.	0.3	0.02	0	11	6	11

reperfusion for 15 min							reperfusion for 30 min						
0% H <sub>2</sub>							0% H <sub>2</sub>						
No.	temp. (°C)	pH	pCO <sub>2</sub>	pO <sub>2</sub>	glucose (mg/dl)	pressure (mmHg)	No.	temp. (°C)	pH	pCO <sub>2</sub>	pO <sub>2</sub>	glucose (mg/dl)	pressure (mmHg)
1	37.3	7.39	45	101	132	155	1	37.5	7.41	41	110	135	140
2	37.2	7.40	52	94	108	135	2	37.4	7.40	49	97	111	130
3	37.3	7.46	44	105	113	135	3	37.0	7.40	51	109	115	118
4	37.5	7.43	46	119	116	153	4	37.5	7.42	46	99	118	135
5	37.2	7.40	44	122	104	155	5	37.1	7.43	40	134	105	130
6	37.7	7.41	43	107	105	140	6	37.7	7.35	50	93	97	110
Average	37.4	7.42	46	108	113	146	Average	37.4	7.40	46	107	114	127
S.D.	0.2	0.03	3	11	10	10	S.D.	0.3	0.03	5	15	13	11
2% H <sub>2</sub>							2% H <sub>2</sub>						
1	37.5	7.42	42	107	120	120	1	37.4	7.39	45	116	115	100
2	37.5	7.41	45	98	100	95	2	37.4	7.43	42	97	103	90
3	37.2	7.40	46	109	111	150	3	37.0	7.38	48	117	112	150
4	37.4	7.39	49	100	110	108	4	37.3	7.36	53	109	110	110
5	37.3	7.40	45	108	107	130	5	37.5	7.37	46	119	107	95
6	37.1	7.39	49	113	105	130	6	37.2	7.38	51	115	109	125
Average	37.3	7.40	46	106	109	122	Average	37.3	7.39	48	112	109	112
S.D.	0.2	0.01	3	6	7	19	S.D.	0.18	0.02	4	8	4	23
4% H <sub>2</sub>							4% H <sub>2</sub>						
1	37.4	7.39	49	103	111	140	1	37.1	7.43	37	142	107	125
2	37.3	7.36	49	93	96	120	2	37.4	7.29	41	133	96	112
3	37.4	7.39	46	90	92	135	3	37.5	7.39	47	93	90	135
4	37.4	7.41	45	113	96	145	4	37.4	7.39	45	134	100	130
5	37.1	7.43	45	107	98	140	5	37.1	7.40	44	138	100	125
6	37.3	7.42	44	120	97	150	6	37.1	7.40	47	143	94	140
Average	37.3	7.40	46	104	98	138	Average	37.3	7.38	44	131	98	128
S.D.	0.12	0.03	2	12	7	10	S.D.	0.19	0.05	4	19	6	10